Energy Surfaces of Carbon Monoxide

Last revision: February 23, 2022

Tutor: Vishal Kumar Sharma (alternative contact person: Eberhard Engel)
Room number: 01.121 (01.122)
Phone number: 798 - 47847 (798 - 47351)
Email: vksharma@itp.uni-frankfurt.de (engel@itp.uni-frankfurt.de)

Contents

1 Goal of Simulation

This simulation aims at an understanding of chemical bonds and some standard methods used for the discussion of the electronic structure of molecules and solids.

2 Born-Oppenheimer Approximation

The standard Hamiltonian for the discussion of electronic structure is given by

$$\hat{H} = \hat{T}_{\rm n} + \hat{H}_{\rm e} \tag{2.1}$$
$$\hat{H}_{\rm e} = \hat{T}_{\rm e} + \hat{V}_{\rm n-e} + \hat{V}_{\rm e-e} + \hat{V}_{\rm n-n} \; . \tag{2.2}$$

Here $\hat{T}_{\rm n}$ represents the kinetic energy of the (K) ions (nuclei) of the system,

$$\hat{T}_{\rm n} = \sum_{\alpha=1}^{K} \frac{(-i\hbar \boldsymbol{\nabla}_{\boldsymbol{R}_\alpha})^2}{2M_\alpha} \; , \tag{2.3}$$

where $\boldsymbol{\nabla}_{\boldsymbol{R}_\alpha}$ abbreviates the gradient with respect to the coordinates $\boldsymbol{R}_\alpha$ of the ion α (with mass M_α). The second component of $\hat{H}$ is the electronic Hamiltonian $\hat{H}_{\rm e}$. Its first contribution is the kinetic energy of the (N) electrons,

$$\hat{T}_{\rm e} = \sum_{i=1}^{N} \frac{(-i\hbar \boldsymbol{\nabla}_i)^2}{2m} \; , \tag{2.4}$$

where the gradient with respect to the position $\boldsymbol{r}_i$ of the i-th electron has been expressed as $\boldsymbol{\nabla}_i$. $\hat{V}_{\rm n-e}$ represents the interaction between electrons and ions (with charges $Z_\alpha e$ — the convention $e = |e|$ is used throughout this text),

$$\hat{V}_{\rm n-e} = -\sum_{\alpha=1}^{K} \sum_{i=1}^{N} \frac{Z_\alpha e^2}{|\boldsymbol{R}_\alpha - \boldsymbol{r}_i|} \; , \tag{2.5}$$

and $\hat{V}_{\rm e-e}$ denotes the interaction between the electrons,

$$\hat{V}_{\rm e-e} = \sum_{i<j=1}^{N} \frac{e^2}{|\boldsymbol{r}_i - \boldsymbol{r}_j|} = \frac{1}{2} \sum_{i,j=1; i\neq j}^{N} \frac{e^2}{|\boldsymbol{r}_i - \boldsymbol{r}_j|} \; . \tag{2.6}$$

Finally, $\hat{H}_{\rm e}$ contains the repulsion between the ions,

$$\hat{V}_{\rm n-n} = \sum_{\alpha<\beta=1}^{K} \frac{Z_\alpha Z_\beta e^2}{|\boldsymbol{R}_\alpha - \boldsymbol{R}_\beta|} = \frac{1}{2} \sum_{\alpha,\beta=1; \alpha\neq\beta}^{K} \frac{Z_\alpha Z_\beta e^2}{|\boldsymbol{R}_\alpha - \boldsymbol{R}_\beta|} \; . \tag{2.7}$$

For the electronic problem $\hat{V}_{\rm n-n}$ just represents an additive constant, which is included in $\hat{H}_{\rm e}$ only for convenience.

The observables one is ultimately interested in all depend (in one way or another) on the eigenstates Λ_n of the Hamiltonian (2.1). Unfortunately, the solution of the corresponding Schrödinger equation,

$$\hat{H}\, \Lambda_n = H_n \, \Lambda_n \; , \tag{2.8}$$

is extremely demanding, due to (i) the coupling of the electronic and ionic degrees of freedom and (ii) the sheer number of the degrees of freedom involved. The first step towards a

solution usually is the Born-Oppenheimer (BO) approximation. Relying on the different time scales of the electronic and the ionic motion, the BO approximation decouples the electronic and ionic degrees of freedom (for a more detailed discussion see e.g. [1] or [2]). In the BO approximation the eigenstates of the Hamiltonian (2.1) are factorized into an ionic wavefunction φ_{ik} and an electronic wavefunction Ψ_k,

$$\Lambda_{ik}(\boldsymbol{X};\boldsymbol{x}) \;=\; \varphi_{ik}(\boldsymbol{X})\,\Psi_k(\boldsymbol{X};\boldsymbol{x})\;, \tag{2.9}$$

where $\boldsymbol{X}$ abbreviates all ionic coordinates, $\boldsymbol{X} \equiv \{\boldsymbol{R}_1, \ldots \boldsymbol{R}_K\}$, and $\boldsymbol{x}$ all electronic degrees of freedom. The electronic wavefunction depends on the ionic positions only parametrically. It satisfies the Schrödinger equation

$$\hat{H}_{\rm e}\,\Psi_k(\boldsymbol{X};\boldsymbol{x}) \;=\; E_k(\boldsymbol{X})\,\Psi_k(\boldsymbol{X};\boldsymbol{x})\;, \tag{2.10}$$

which is a stationary eigenvalue problem for any given set $\{\boldsymbol{R}_1, \ldots \boldsymbol{R}_K\}$. For given electronic state k, the eigenvalue $E_k(\boldsymbol{X})$ then acts as the potential in which the ions are moving,

$$\left\{\hat{T}_{\rm n} + E_k(\boldsymbol{X})\right\}\varphi_{ik}(\boldsymbol{X}) \;=\; H_{ik}\,\varphi_{ik}(\boldsymbol{X})\,, \tag{2.11}$$

so that, at least in principle, Eq.(2.10) has to be solved for all possible arrangements $\{\boldsymbol{R}_1, \ldots \boldsymbol{R}_K\}$ of the ions. $E_k(\boldsymbol{X})$ is often called the BO energy surface or BO potential, or simply the energy surface. When plotting and analyzing this quantity, usually the ground state energies of the constituent atoms are subtracted,

$$E_k^{\rm BO}(\boldsymbol{X}) \;=\; E_k(\boldsymbol{X}) - \sum_{\alpha=1}^{K} E_\alpha^{\rm atom}\,, \tag{2.12}$$

where $E_\alpha^{\rm atom}$ is the ground state energy of the isolated constituent atom α. As a result of the BO approximation, the molecular state (2.9), i.e. the state of the coupled system of electrons and ions, and its eigenenergy H_{ik} depend on both the state k in which the electrons are and the associated state i of the ions.

3 Density Functional Theory

3.1 Basics

This section provides the theoretical background for the method used in the program package DIAMOL for the solution of the many-electron problem (2.10).

Within the Born-Oppenheimer approximation the standard Hamiltonian of a stationary many-electron system is given by Eq.(2.2), in which, however, the additive constant $\hat{V}_{\rm n-n}$ is usually dropped as long as only the electronic problem is considered. The many-electron eigenstates Ψ_k corresponding to $\hat{H}_{\rm e}$ are obtained by solution of the Schrödinger equation (2.10) for any given set $\{\boldsymbol{R}_1, \ldots \boldsymbol{R}_K\}$. However, even in the case of the ground state Ψ_0, on which we will focus in the following, the solution of Eq.(2.10) is highly non-trivial. In fact, an (essentially) exact solution is only available for the ground states of rather simple systems, such as the Helium atom or the Hydrogen dimer. While extremely accurate $|\Psi_k\rangle$

can still be obtained for molecules of moderate size or high symmetry, approximations are necessary as soon as the number of atoms involved increases.

For a large variety of molecular and condensed matter systems effective single-particle approaches turn out to give reasonably accurate results for many ground state observables of interest. The most well-known approach of this type is the Hartree-Fock (HF) method, which is obtained by approximating the ground state in terms of a (Slater) determinant of single-particle states,

$$\Psi_0(\boldsymbol{r}_1\sigma_1,\ldots\boldsymbol{r}_N\sigma_N) \;\approx\; \frac{1}{\sqrt{N!}}\det\begin{pmatrix} \phi_1(\boldsymbol{r}_1\sigma_1) & \cdots & \phi_N(\boldsymbol{r}_1\sigma_1) \\ \vdots & & \vdots \\ \phi_1(\boldsymbol{r}_N\sigma_N) & \cdots & \phi_N(\boldsymbol{r}_N\sigma_N) \end{pmatrix} \quad . \tag{3.1}$$

Here σ_i denotes the spin-variable of the i-th electron — the spin degree of freedom has been expressed explicitly in terms of the variable σ, rather than by understanding all wavefunctions involved as spinors. Correspondingly, σ_i denotes the spin-variable of the i-th electron. The single-particle states $\phi_i(\boldsymbol{r}\sigma)$ in (3.1) are the N energetically lowest solutions of the HF equations. In these equations each electron experiences the same average potential, which, in addition to the ionic potential, contains the direct Coulomb repulsion between the electrons and an exchange (Fock) component which reflects the Pauli exclusion principle.

The HF approximation misses, however, all correlation contributions: neither the state (3.1) and the corresponding total HF energy nor the average single-particle potential account for the so-called Coulomb correlation, i.e. the fact that, at any instant of time, an electron recognizes all other electrons at exactly the positions where they are. This deficiency is partially overcome by the currently most often used effective single-particle approach, density functional theory (DFT).

DFT is based on the observation that the ground state Ψ_0 of a many-particle system is uniquely determined by the associated ground state 1-particle density,

$$n_0(\boldsymbol{r}) \;=\; N\sum_{\sigma_1,\ldots\sigma_N}\int d^3r_2\ldots d^3r_N\,|\Psi_0(\boldsymbol{r}\sigma_1,\boldsymbol{r}_2\sigma_2\ldots\boldsymbol{r}_N\sigma_N)|^2\;. \tag{3.2}$$

The density $n_0(\boldsymbol{r})$ is characteristic of the ground state Ψ_0 and thus of the ionic potential experienced by the electrons: two different ionic potentials lead to two different Ψ_0 which, in turn, yield two different $n_0(\boldsymbol{r})$ and vice versa (as long as the ground states are non-degenerate — which we will always assume in the following). Mathematically speaking, the ground state is a unique functional of the ground state density, $\Psi[n]$, with $\Psi_0=\Psi[n_0]$. This result allows to understand the ground state energies

$$E_0 \;=\; \langle\Psi_0|\hat{H}_{\rm e}|\Psi_0\rangle$$

obtained for all possible ionic potentials as a unique functional of the corresponding ground state densities,

$$E[n] \;=\; \langle\Psi[n]|\hat{H}_{\rm e}|\Psi[n]\rangle \qquad \text{with} \qquad E_0 \;=\; E[n_0]\;,$$

and the same is true for the various components of E_0. Moreover, one can show by use of the Ritz variational principle that, for given ionic potential, the functional $E[n]$ is minimized by the density $n_0(\boldsymbol{r})$ which corresponds to this ionic potential. The solution of the Schrödinger

equation (2.10) for the ground state has thus been recast as a minimization problem for the energy functional $E[n]$. (for a more detailed and mathematically more careful discussion of DFT see [1] or [3]).

3.2 Kohn-Sham equations

On this basis one can then map the full electronic problem (2.10) onto an effective single-particle problem with a ground state of the form (3.1), such that this effective single-particle problem has the same $n_0(\boldsymbol{r})$ as the original interacting system. The single-particle states of this so-called Kohn-Sham (KS) system satisfy the KS equation,

$$\left\{ -\frac{\hbar^2 \boldsymbol{\nabla}^2}{2m} + v_{\rm s}(\boldsymbol{r}) \right\} \phi_i(\boldsymbol{r}\sigma) \;\; = \;\; \epsilon_i \, \phi_i(\boldsymbol{r}\sigma) \, . \tag{3.3}$$

Here the states are again assumed to be ordered with respect to their eigenenergies ϵ_i,

$$\epsilon_1 \leq \ldots \leq \epsilon_N < \epsilon_{N+1} \leq \ldots \tag{3.4}$$

(i represents both spatial and spin quantum numbers). The density corresponding to the KS ground state (3.1) is given by

$$n(\boldsymbol{r}) = \sum_{\sigma=\uparrow,\downarrow} \sum_{i=1}^{N} |\phi_i(\boldsymbol{r}\sigma)|^2 = \sum_{\sigma=\uparrow,\downarrow} \sum_{i} \Theta_i \, |\phi_i(\boldsymbol{r}\sigma)|^2 \, , \tag{3.5}$$

where the occupation function Θ_i has been introduced (and the index 0 at n has been dropped for brevity). In the present situation, Θ_i is the standard step function,

$$\Theta_i \equiv \left\{ \begin{array}{ll} 1 & \text{for} \;\; \epsilon_i \leq \epsilon_N \\ 0 & \text{else} \end{array} \right. \, . \tag{3.6}$$

The formulation (3.5) has, however, the advantage that it can be easily generalized to degenerate and excited states as well as to systems at finite temperature. The effective single-particle potential $v_{\rm s}$ is given by

$$v_{\rm s}(\boldsymbol{r}) \;\; = \;\; v_{\rm n-e}(\boldsymbol{r}) + v_{\rm H}[n](\boldsymbol{r}) + v_{\rm xc}[n](\boldsymbol{r}) \, . \tag{3.7}$$

Here $v_{\rm n-e}$ denotes the total ionic potential,

$$v_{\rm n-e}(\boldsymbol{r}) \;\; = \;\; -\sum_{\alpha=1}^{K} \frac{Z_\alpha e^2}{|\boldsymbol{R}_\alpha - \boldsymbol{r}|} \, , \tag{3.8}$$

and the Hartree potential $v_{\rm H}$ provides the electrostatic repulsion between the electrons,

$$v_{\rm H}[n](\boldsymbol{r}) \;\; = \;\; e^2 \int d^3r' \, \frac{n(\boldsymbol{r'})}{|\boldsymbol{r} - \boldsymbol{r'}|} \, . \tag{3.9}$$

Finally, the so-called exchange-correlation (xc) potential $v_{\rm xc}$ is defined as

$$v_{\rm xc}[n](\boldsymbol{r}) \;\; = \;\; \frac{\delta E_{\rm xc}[n]}{\delta n(\boldsymbol{r})} \, . \tag{3.10}$$

It inherits all xc-effects from the so-called xc-energy functional $E_{\rm xc}[n]$. In order to define this quantity, one expresses the total energy of the interacting system as

$$E[n] \;=\; T_{\rm s}[n] + E_{\rm n-e}[n] + E_{\rm H}[n] + E_{\rm xc}[n]\,, \tag{3.11}$$

where it has been indicated that not only E but also its components are functionals of the density. $T_{\rm s}$ represents the kinetic energy of the KS particles,

$$T_{\rm s} \;=\; \sum_i \Theta_i \sum_{\sigma=\uparrow,\downarrow} \int d^3r\, \phi_i^*(\boldsymbol{r}\sigma) \frac{(-i\hbar\boldsymbol{\nabla})^2}{2m} \phi_i(\boldsymbol{r}\sigma)\,, \tag{3.12}$$

for which the explicit dependence on n is neither known nor required. $E_{\rm n-e}[n]$ is the electron-ion interaction energy,

$$E_{\rm n-e}[n] \;=\; \int d^3r\, v_{\rm n-e}(\boldsymbol{r})\, n(\boldsymbol{r})\,. \tag{3.13}$$

$E_{\rm H}[n]$ represents the electrostatic energy of the electron charge distribution,

$$E_{\rm H}[n] \;=\; \frac{e^2}{2} \int d^3r \int d^3r'\, \frac{n(\boldsymbol{r})n(\boldsymbol{r}')}{|\boldsymbol{r}-\boldsymbol{r}'|}\,, \tag{3.14}$$

including their self-interaction energy. $E_{\rm H}[n]$ is usually referred to as Hartree term. Finally, $E_{\rm xc}[n]$ is defined by Eq.(3.11). It absorbs all the many-body effects not contained in $T_{\rm s}$, $E_{\rm H}$ and $E_{\rm ext}$, most notably the Fock exchange energy of the electrons. However, it also contains the Coulomb correlation effects not present in the HF approximation. So, while the KS ground state (3.1) is uncorrelated (i.e. determinantal) just as the HF ground state, the DFT energy (3.11) and the KS single-particle potential (3.7) do contain correlation contributions.

Taking Eqs.(3.5)–(3.14) together, one realizes that $v_{\rm s}$ depends on the solutions of Eq.(3.3), so that this equation has to be solved in a self-consistent fashion, similar to the HF equation. One starts with some trial density $n^{(1)}$ which allows to construct starting potentials $v_{\rm H}[n^{(1)}](\boldsymbol{r})$ and $v_{\rm xc}[n^{(1)}](\boldsymbol{r})$ (assuming $E_{\rm xc}[n]$ to be given). Solution of (3.3) then provides some orbitals $\phi_i^{(2)}$ which lead to an improved density $n^{(2)}$ via Eq.(3.5). The density $n^{(2)}$ can be used to obtain improved potentials $v_{\rm H}[n^{(2)}](\boldsymbol{r})$ and $v_{\rm xc}[n^{(2)}](\boldsymbol{r})$. This iterative procedure is repeated until the maximum difference between the densities (or potentials) obtained in two successive iterations falls below some predefined accuracy criterion.

3.3 Exchange-correlation energy functional

The decomposition (3.11) extracts exactly those contributions to the total energy functional, which can be treated rigorously: $E_{\rm H}$ and $E_{\rm ext}$ are simple functionals of the density whose evaluation is straightforward. $T_{\rm s}$ is the kinetic energy of the KS system which can be easily evaluated from (3.12). At the same time, these ingredients of $E[n]$ usually dominate the physics of the system. Sometimes even the complete neglect of $E_{\rm xc}$ leads to an electronic structure which is qualitatively correct. One would thus hope that an approximate account of $E_{\rm xc}$ is sufficient for an accurate description of many systems.

Given the fact that one does not even know $T_{\rm s}$ as a functional of n, one might still be sceptical that a suitable approximation for $E_{\rm xc}[n]$ can be found. However, there exists a prominent interacting many-body system for which the density-dependence of the xc-energy is very well known, the homogeneous (or uniform) electron gas (HEG). The HEG is a system of infinitely many interacting electrons (distributed over all space) which do not experience a spatially varying ionic potential. If the number of electrons per volume exceeds a certain threshold, the ground state density n_0 of the HEG is constant throughout all space, i.e. homogeneous. Of course, the total energy of infinitely many particles is infinite, only the energy density is a meaningful quantity, or, alternatively, the energy per particle. In fact, due to the long range of the Coulomb interaction, even the energy density of infinitely many electrons diverges. In order to resolve this problem, the charge of the electrons has to be neutralized by a homogeneous ionic background charge density. As a result the net charge in any suitably chosen volume of space is zero, so that the long-range Coulomb forces vanish and a finite energy density is obtained.

The xc-energy density $e_{\rm xc}$ of the HEG is a simple function of n_0, rather than a full functional. Its exchange contribution is given by

$$e_{\rm x}^{\rm HEG}(n_0) \;=\; -\frac{3(3\pi^2)^{1/3}}{4\pi}\, e^2\, n_0^{4/3}\;. \tag{3.15}$$

An analytical calculation of the correlation contribution is only possible in the high- and low-density limits. One has to resort to Monte-Carlo simulations in order to extract the information on the (physically most relevant) regime of intermediate densities. The resulting numerical data have been combined with the analytically known high- and low-density limits in accurate parameterizations. Several such parameterizations of $e_{\rm c}(n_0)$ are available in the literature. Some up-to-date examples are shown in Fig. 1.

It remains to convert $e_{\rm xc}(n_0)$ into a density functional which can be used for realistic electronic structure calculations. This goal is achieved by the local density approximation (LDA). In the LDA the xc-energy density of the actual, inhomogeneous system with local density $n(\boldsymbol{r})$ is locally approximated by the xc-energy density of an electron gas with constant density $n_0 = n(\boldsymbol{r})$,

$$E_{\rm xc}^{\rm LDA}[n] \;=\; \int d^3r\, e_{\rm xc}^{\rm HEG}(n(\boldsymbol{r}))\;. \tag{3.16}$$

The LDA can be applied to arbitrarily inhomogeneous systems without encountering any technical difficulties, since the corresponding xc-potential is a simple function of the local density. For instance, for the exchange component one finds

$$v_{\rm x}^{\rm LDA}(\boldsymbol{r}) = \frac{\delta E_{\rm x}^{\rm LDA}[n]}{\delta n(\boldsymbol{r})} = \left.\frac{de_{\rm x}^{\rm HEG}(n_0)}{dn_0}\right|_{n_0=n(\boldsymbol{r})} = -e^2\,\frac{[3\pi^3 n(\boldsymbol{r})]^{1/3}}{\pi}\;. \tag{3.17}$$

However, the LDA treats any system locally as an electron gas, so that its technical applicability should not be misinterpreted as validity. In fact, given its origin one would expect the LDA to be useful only for systems which resemble some of the properties of the HEG, as for instance simple metals. In practice, the LDA turns out to be surprisingly accurate for many rather inhomogeneous systems.

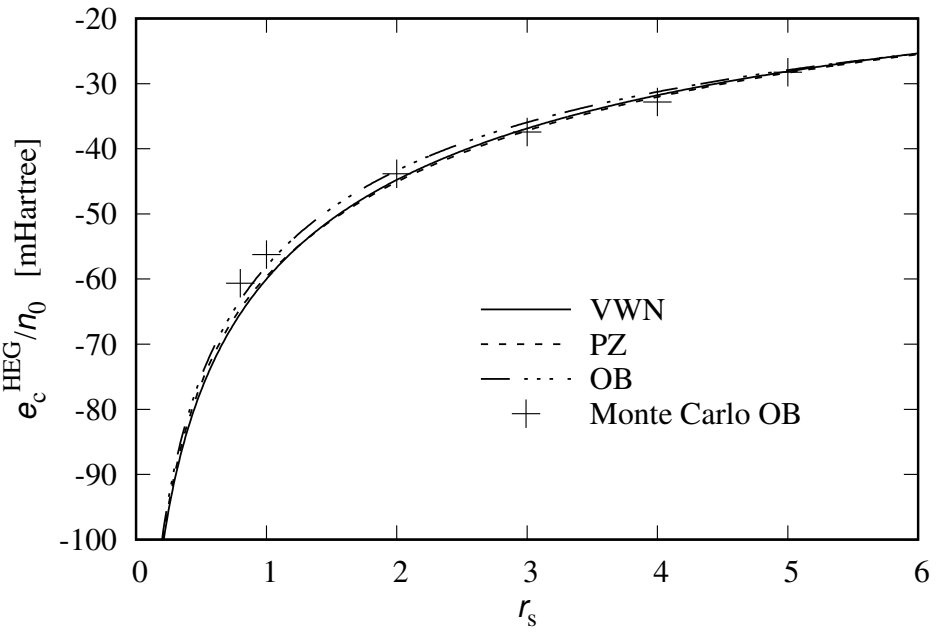

Figure 1: Correlation energy per electron ($e_{\rm c}^{\rm HEG}/n_0$) of the spin-saturated homogeneous electron gas as a function of the Wigner-Seitz radius $r_{\rm s} = (\frac{3}{4\pi n_0})^{1/3}/a_0$ ($r_{\rm s}$ is the dimensionless ratio between the radius of the sphere which is on average occupied by a single electron of the gas and the Bohr radius $a_0 = \hbar^2/(me^2)$) for several parameterizations: VWN [4], PZ [5], OB [6]. Also given are the original Monte-Carlo data [6].

Several classes of improved xc-functionals have been developed over time. Today, the workhorse in DFT calculations is the so-called generalized gradient approximation (GGA), in which the simple dependence of $E_{\rm xc}^{\rm LDA}$ on the density is augmented by a dependence on the first (or even the second) gradient of n. More ambitious approximations involve a fully nonlocal dependence on the density. Quite a number of flavors of both classes of functionals exist in the literature, a discussion of which is beyond the scope of this brief introduction (see e.g. [3]).

3.4 Exited states

So far, the complete DFT formalism is restricted to the ground state, since the prime argument underlying DFT is the energy minimum principle. However, such a variational principle is also available for individual sectors of the many-electron Hilbert space, if a symmetry of the Hamiltonian allows to distinguish the sectors rigorously. For the Hamiltonian (2.2) this is, for instance, the case for the projection of the total spin on the z-axis, $\hat{S}_z$. Since the Hamiltonian (2.2) commutes with $\hat{S}_z$,

$$\left[\hat{H}_{\rm e}, \hat{S}_z\right] \;=\; 0 \qquad \text{with} \qquad \hat{S}_z \;=\; \sum_{i=1}^{N} \hat{s}_z \;=\; \sum_{i=1}^{N} \sigma_{i,z} \tag{3.18}$$

(the Pauli matrix $\sigma_{i,z}$ acts on the spin-variable of the i-th electron,[1] the prefactor $\hbar/2$ has been dropped for convenience), all states Ψ_k, and in particular the ground state (3.1), can be chosen to be eigenstates of both operators simultaneously,

$$\hat{S}_z \, \Psi_k \;\; = \;\; S_k \, \Psi_k \; . \tag{3.19}$$

While the ground state of the system corresponds to one particular eigenvalue S_0 of $\hat{S}_z$, states with $S_k \neq S_0$ have zero overlap with the ground state. Consequently, energy minimization for fixed $S_k \neq S_0$ does not lead to a collapse to the global ground state, but rather to the lowest energy state for the S_k given. Sometimes spatial symmetries of the system introduce additional quantum numbers (such as angular momentum) with respect to which the Hilbert space can be decomposed. Once there exists a minimum principle for some sector, the DFT scheme can be applied to it. In this way, one can establish a DFT treatment for certain classes of excited states.

For convenience we note that the eigenvalue S_k can be combined with the total number of electrons to the number of electrons with spin σ, N_σ,

$$\frac{1}{2}\left(\hat{N} + \hat{S}_z\right) \Psi_k \;\; = \;\; \frac{1}{2}(N + S_k)\Psi_k \;\; = \;\; N_\uparrow \, \Psi_k \tag{3.20}$$

$$\frac{1}{2}\left(\hat{N} - \hat{S}_z\right) \Psi_k \;\; = \;\; \frac{1}{2}(N - S_k)\Psi_k \;\; = \;\; N_\downarrow \, \Psi_k \; . \tag{3.21}$$

The states Ψ_k can therefore alternatively be classified by $N_\uparrow, N_\downarrow$. Moreover, in the case of determinantal states such as (3.1) the independence of the Hamiltonian of spin implies that one can factorize the single-particle orbitals as

$$\phi_i(\boldsymbol{r}\sigma) \;\; = \;\; \phi_{\alpha s}(\boldsymbol{r}) \, \chi_s(\sigma) \qquad\qquad (i \equiv \alpha s) \; , \tag{3.22}$$

where χ_s denotes the Pauli spinors (in the notation for the spin variable chosen),

$$\chi_s(\sigma) \;\; = \;\; \delta_{s\sigma} \qquad\qquad \chi_\uparrow = \begin{pmatrix} 1 \\ 0 \end{pmatrix} \qquad\qquad \chi_\downarrow = \begin{pmatrix} 0 \\ 1 \end{pmatrix} \; . \tag{3.23}$$

3.5 Spin-density functional theory

The complete formalism sketched out so far can be extended to systems subject to additional (external) magnetic fields.[2] In this extended formalism, termed spin-density functional theory (SDFT), the ground state spin-densities $n_\uparrow$ and $n_\downarrow$,

$$n_\sigma(\boldsymbol{r}) \;\; = \;\; N \sum_{\sigma_2, \ldots \sigma_N} \int d^3 r_2 \ldots d^3 r_N \, |\Psi_0(\boldsymbol{r}\sigma, \boldsymbol{r}_2\sigma_2 \ldots \boldsymbol{r}_N\sigma_N)|^2 \; , \tag{3.24}$$

[1] The Pauli matrix σ_z is given by

$$\sigma_z \;\; = \;\; \begin{pmatrix} 1 & 0 \\ 0 & -1 \end{pmatrix} \; .$$

[2] For simplicity, the discussion is here restricted to magnetic fields which point into the same direction throughout all space.

play the same role as the density n plays in the formalism without magnetic field. It turns out that application of SDFT is also advantageous if there is no external magnetic field: SDFT allows to account for the spin-dependence of $E_{\rm xc}$ in a rigorous fashion, which is not possible by a functional of the total density n. This aspect is of crucial importance for all systems with a non-zero magnetic moment, such as open-shell atoms and molecules or ferromagnetic solids.

The KS equation of SDFT is given by

$$\left\{ -\frac{\hbar^2 \boldsymbol{\nabla}^2}{2m} + v_{\rm s}^{\sigma}[n_\uparrow, n_\downarrow](\boldsymbol{r}) \right\} \phi_{\alpha\sigma}(\boldsymbol{r}) \;=\; \epsilon_{\alpha\sigma}\, \phi_{\alpha\sigma}(\boldsymbol{r}) \;, \tag{3.25}$$

with the KS potential decomposed in similar manner as in (3.7),

$$v_{\rm s}^{\sigma}[n_\uparrow, n_\downarrow](\boldsymbol{r}) \;=\; v_{\rm n-e}(\boldsymbol{r}) + v_{\rm H}[n](\boldsymbol{r}) + v_{\rm xc}^{\sigma}[n_\uparrow, n_\downarrow](\boldsymbol{r}) \;. \tag{3.26}$$

$v_{\rm n-e}$ and $v_{\rm H}$ are still given by Eqs.(3.8) and (3.9), respectively. The total density required for Eq.(3.9) is obtained as the sum of the two spin-contributions,

$$n(\boldsymbol{r}) \;=\; n_\uparrow(\boldsymbol{r}) + n_\downarrow(\boldsymbol{r}) \tag{3.27}$$

$$n_\sigma(\boldsymbol{r}) \;=\; \sum_\alpha \Theta_{\alpha\sigma} |\phi_{\alpha\sigma}(\boldsymbol{r})|^2 \,. \tag{3.28}$$

For both spin-channels the energetically lowest $\phi_{\alpha\sigma}$ are occupied (in the case of the ground state). However, the number N_σ of electrons with spin σ is only restricted by the total number of electrons, N,

$$N \;=\; N_\uparrow + N_\downarrow \,. \tag{3.29}$$

Within this restriction, the occupation of each spin can be chosen freely, since each pair of $N_\uparrow, N_\downarrow$ defines a seperate sector (with total spin-projection $S = N_\uparrow - N_\downarrow$) of the N-electron Hilbert space for which the Ritz variational principle and thus SDFT is valid. For given $N_\uparrow, N_\downarrow$ the occupation numbers are thus given by

$$\Theta_{\alpha\sigma} \;=\; \begin{cases} 1 & \text{for } \epsilon_{\alpha\sigma} \le \epsilon_{N_\sigma} \\ 0 & \text{for } \epsilon_{\alpha\sigma} > \epsilon_{N_\sigma} \end{cases} \quad \text{with} \quad \textstyle\sum_\alpha \Theta_{\alpha\sigma} = N_\sigma \;, \quad . \tag{3.30}$$

The spin-dependent xc-potential is obtained as functional derivative of the xc-energy functional $E_{\rm xc}[n_\uparrow, n_\downarrow]$ of SDFT,

$$v_{\rm xc}^{\sigma}[n_\uparrow, n_\downarrow](\boldsymbol{r}) \;=\; \frac{\delta E_{\rm xc}[n_\uparrow, n_\downarrow]}{\delta n_\sigma(\boldsymbol{r})} \,, \tag{3.31}$$

which, in turn, is defined by an appropriate decomposition of the total energy,

$$E[n_\uparrow, n_\downarrow] \;=\; T_{\rm s}[n_\uparrow, n_\downarrow] + E_{\rm n-e}[n] + E_{\rm H}[n] + E_{\rm xc}[n_\uparrow, n_\downarrow] \tag{3.32}$$

$$T_{\rm s}[n_\uparrow, n_\downarrow] \;=\; \sum_{\sigma=\uparrow,\downarrow} \sum_\alpha \Theta_{\alpha\sigma} \int d^3r\, \phi_{\alpha\sigma}^*(\boldsymbol{r}) \frac{(-i\hbar\boldsymbol{\nabla})^2}{2m} \phi_{\alpha\sigma}(\boldsymbol{r}) \,. \tag{3.33}$$

The concept of the LDA can also be extended to SDFT, relying on the xc-energy density $e_{\rm xc}^{\rm HEG}(n_\uparrow, n_\downarrow)$ of a spin-polarized HEG with gas densities $n_{0,\uparrow} \neq n_{0,\downarrow}$. The local spin-density approximation (LSDA) is then defined as

$$E_{\rm xc}^{\rm LSDA}[n_\uparrow, n_\downarrow] = E_{\rm x}^{\rm LSDA}[n_\uparrow, n_\downarrow] + E_{\rm c}^{\rm LSDA}[n_\uparrow, n_\downarrow] \tag{3.34}$$

$$E_{\rm x}^{\rm LSDA}[n_\uparrow, n_\downarrow] = -\frac{3(6\pi^2)^{1/3}}{4\pi}\, e^2 \sum_{\sigma=\uparrow,\downarrow} \int d^3r\, n_\sigma^{4/3}(\boldsymbol{r}) \tag{3.35}$$

$$E_{\rm c}^{\rm LSDA}[n_\uparrow, n_\downarrow] = \int d^3r\, e_{\rm c}^{\rm HEG}\left(n_\uparrow(\boldsymbol{r}), n_\downarrow(\boldsymbol{r})\right) \tag{3.36}$$

In the following, we will no longer distinguish between LDA and LSDA: the term LDA should automatically be understood as LSDA whenever spin-polarization is present.

4 Diatomic Molecules

In the case of diatomic molecules the ionic potential (3.8) can be written as[3]

$$v_{\rm n-e}(\boldsymbol{r}) = -\frac{Z_1}{|\boldsymbol{r} + (0,0,R/2)|} - \frac{Z_2}{|\boldsymbol{r} - (0,0,R/2)|}\,, \tag{4.1}$$

where the two nuclei with internuclear separation R have been chosen to sit on the z-axis at distances $\pm R/2$ from the origin (compare Fig. 2). For convenience the quantity $R/2$ will be abbreviated by f in the following.

Due to the rotational symmetry of $v_{\rm n-e}$ with respect to the z-axis the solutions of (3.25) can be classified by the corresponding angular momentum projection quantum number m. One can thus factorize the eigenstates as

$$\phi_{\alpha\sigma}(\boldsymbol{r}) = \bar{\phi}_{jm\sigma}(\rho, z)\, e^{im\varphi} \quad , \quad m = 0, \pm 1, \pm 2, \ldots \quad , \tag{4.2}$$

where, for the moment, cylindrical coordinates ρ, φ, z have been used for $\bar{\phi}_{jm\sigma}$. The integer $j = 1, 2, \ldots$ denotes the sequence of levels for given m, which are again assumed to be energetically ordered. The molecular single-particle orbitals are denoted as $\sigma, \pi, \delta, \varphi, \ldots$-states for $|m| = 0, 1, 2, 3, \ldots$, respectively.

Similarly, the N-electron ground state of a diatomic molecule can be classified in terms of the total angular momentum projection Λ and the total spin projection S (see e.g. [7,2]). In the case of the Slater determinant (3.1) these quantities can be expressed in terms of the angular momentum projections m of the individual states of type (4.2) in the determinant and the spin projections σ which are multiplied with them according to (3.22),

$$\Lambda = \sum_{m=-\infty}^{\infty} m \sum_{\sigma=\uparrow,\downarrow} \sum_{j=1}^{\infty} \Theta_{jm\sigma}\,, \tag{4.3}$$

$$S = \frac{1}{2} \sum_{m=-\infty}^{\infty} \left[\sum_{j=1}^{\infty} \Theta_{jm\uparrow} - \sum_{j=1}^{\infty} \Theta_{jm\downarrow} \right] = \frac{1}{2}\left(N_\uparrow - N_\downarrow\right)\,. \tag{4.4}$$

[3]From now on atomic units $\hbar = m = e^2 = 1$ will be used.

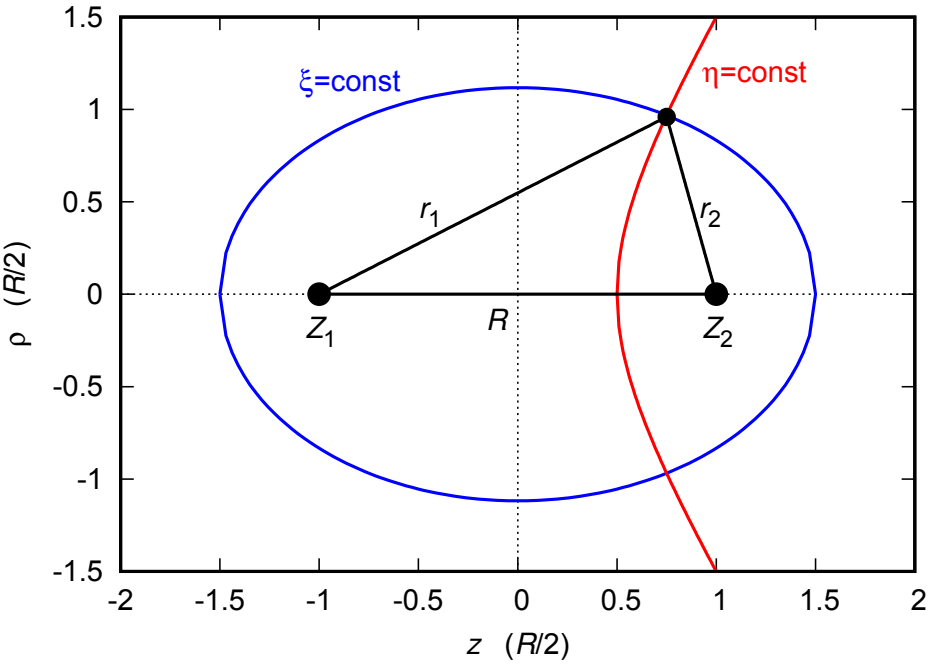

Figure 2: Geometry of two-center problem.

The standard labelling of the N-electron states is ${}^{2S+1}\Lambda$, with $\Lambda = 0, 1, 2, 3, \ldots$ expressed in terms of upper case greek letters as $\Sigma, \Pi, \Delta, \Phi, \ldots$, respectively. Obviously, for any state with $\Lambda > 0$ there is an energetically degenerate state with angular momentum $-\Lambda$, which is, however, not distinguished from the state with $\Lambda > 0$.

The potential (4.1) is not only axially symmetric, it is also symmetric under inversion with respect to any plane which contains the interatomic axis. As a consequence, Σ-states can either change sign under this inversion or not (since a second inversion leads back to the original state). Accordingly, they are labelled as Σ^- or Σ^+ states. In the case of states with $\Lambda \neq 0$ the inversion with respect to a plane containing the interatomic axis just transforms the state with $\Lambda > 0$ into the state $-\Lambda$ and vice versa.[4]

If, in addition, $Z_1 = Z_2$ one also has inversion symmetry with respect to $z \to -z$, so that the states are either even or odd under this transformation, which is indicated by a subscript g (gerade) or u (ungerade).[5]

In order to distinguish the electronic ground state from electronic excited states, often an additional letter is used: X denotes the ground state and $A, B, C, \ldots$ label the 1st, 2nd, 3rd, ...excited state, respectively. However, this notation is not strictly met: sometimes

[4]If such a plane has an angle α with respect to the x-axis, inversion with respect to this plane transforms a point with azimuthal angle φ into a point with angle $2\alpha - \varphi$. The phase of a molecular single-particle state thus behaves as

$$e^{im\varphi} \quad \longrightarrow \quad e^{im(2\alpha-\varphi)} = e^{2im\alpha}\, e^{-im\varphi} \,.$$

When summing up the individual contributions according to Eq.(4.3), one thus ends up with $-\Lambda$, while $e^{2im\alpha}$ generates an irrelevant global phase.

[5]This classification is, in fact, used for any axially symmetric problem with an additional inversion symmetry with respect to a plane perpedicular to the axis.

lower case letters or even letters out of the alphabetical order are utilized for the excited states. The ground state of diatomic molecules often is a state with highest symmetry, $\Sigma^+_{(g)}$, which is fully characterized by $X^{2S+1}\Sigma^+_{(g)}$.

The bond types of diatomic molecules can be understood by analysis of the molecular (two-center) orbitals resulting from linear combination of atomic orbitals (LCAO). The latter have s, p, d, ... character. The linear combination of two s-orbitals centered around the nuclei at $\pm f$ is always axially symmetric and thus corresponds to a molecular single-particle state with $m = 0$, i.e. to a σ-orbital. The same is true for the linear combination of two p_z-orbitals, but also for the combination of two d_{z^2}-orbitals and the combinations $s - p_z$, $s - d_{z^2}$, $p_z - d_{z^2}$ etc. All these atomic orbitals with matching axial symmetry hybridize in molecules (provided, they have at least some limited overlap, of course). If the atomic orbitals both correspond to $m = 1$ they can form molecular π-orbitals, if they share a nodal plane which also contains the internuclear axis. Possible combinations are $p_x - p_x$ and $p_y - p_y$, but also the states d_{yz} and d_{zx} could be involved. Finally, a δ-state ($m = 2$) may be formed from the combinations $d_{xy} - d_{xy}$ or $d_{x^2-y^2} - d_{x^2-y^2}$ (in this case the atomic orbitals to be combined have to share two nodal planes which also contain the internuclear axis). If the angular momentum projections of the atomic orbitals do not match, the orbitals are called non-bonding.

Before these bond types are illustrated by some examples, one final characterization of molecular orbitals remains to be introduced. Consider, for simplicity, the ground state of the H_2^+ molecule, i.e. a single electron in the field of two protons. The atomic orbitals in the corresponding molecular ground state are the $1s$-orbitals ϕ_1 and ϕ_2 of the Hydrogen atoms at the positions of the two protons,

$$\left[\hat{T} + \hat{V}_i\right] \phi_i \;=\; \epsilon_i \, \phi_i \;,$$

where $\hat{V}_{1,2}$ represents the potentials of the protons at $\boldsymbol{R}_{1,2} = (0, 0, \pm R/2)$,

$$\hat{V}_1 \;=\; \frac{-1}{|\boldsymbol{r} - \boldsymbol{R}_1|} \qquad\qquad \hat{V}_2 \;=\; \frac{-1}{|\boldsymbol{r} - \boldsymbol{R}_2|} \;.$$

Then two possible linear combinations exist,

$$\Phi_+ \;=\; \frac{1}{\sqrt{2}} \, (\phi_1 + \phi_2) \qquad\qquad \text{and} \qquad\qquad \Phi_- \;=\; \frac{1}{\sqrt{2}} \, (\phi_1 - \phi_2) \;,$$

where all states involved have been assumed to be real (which is always possible for bound states) and both ϕ_1 and ϕ_2 are chosen to be positive (they do not have nodes). Given these choices, Φ_+ is nodeless, while Φ_- has a nodal plane in the middle between the two protons. At first glance, both are candidates for the ground state of H_2^+. However, the two states are quite different in energy. This is most easily understood by using stationary perturbation theory to evaluate the molecular energy for the states $\Phi_\pm$. Combining the states $\Phi_\pm$ with the Hamiltonian for the H_2^+ molecule,

$$\hat{H}_\mathrm{e} \;=\; \hat{T} + \hat{V}_1 + \hat{V}_2 + \hat{V}_\mathrm{n-n} \;,$$

one obtains

$$\begin{aligned}
\langle\Phi_\pm|\Phi_\pm\rangle &= 1 \pm \langle\phi_1|\phi_2\rangle \\
E_\pm &= \frac{\langle\Phi_\pm|\hat{T}+\hat{V}_1+\hat{V}_2|\Phi_\pm\rangle}{\langle\Phi_\pm|\Phi_\pm\rangle} + \frac{Z_1 Z_2}{R} \\
&= \frac{\epsilon_1+\epsilon_2}{2} + \frac{\langle\phi_1|\hat{V}_2|\phi_1\rangle + \langle\phi_2|\hat{V}_1|\phi_2\rangle}{2\left[1 \pm \langle\phi_1|\phi_2\rangle\right]} \pm \frac{\langle\phi_1|\hat{V}_2|\phi_2\rangle + \langle\phi_2|\hat{V}_1|\phi_1\rangle}{2\left[1 \pm \langle\phi_1|\phi_2\rangle\right]} + \frac{Z_1 Z_2}{R} \,. \quad (4.5)
\end{aligned}$$

If the overlap of the two $1s$-orbitals is small, $\langle\phi_1|\phi_2\rangle \ll 1$, one can expand the energy in powers of the overlap. Keeping only the lowest order corrections, one arrives at

$$\begin{aligned}
E_\pm &= \frac{1}{2}\Big\{\epsilon_1+\epsilon_2 + \Big[\langle\phi_1|\hat{V}_2|\phi_1\rangle + \langle\phi_2|\hat{V}_1|\phi_2\rangle\Big]\left[1 \mp \langle\phi_1|\phi_2\rangle\right] \\
&\qquad \pm \Big[\langle\phi_1|\hat{V}_2|\phi_2\rangle + \langle\phi_2|\hat{V}_1|\phi_1\rangle\Big]\left[1 \mp \langle\phi_1|\phi_2\rangle\right]\Big\} + \frac{Z_1 Z_2}{R} \,.
\end{aligned}$$

The difference between the total energies of Φ_+ and $|\Phi_-$ is thus obtained as

$$E_+ - E_- = -\Big[\langle\phi_1|\hat{V}_2|\phi_1\rangle + \langle\phi_2|\hat{V}_1|\phi_2\rangle\Big]\langle\phi_1|\phi_2\rangle + \langle\phi_1|\hat{V}_2|\phi_2\rangle + \langle\phi_2|\hat{V}_1|\phi_1\rangle \,.$$

The potentials $\hat{V}_1$ and $\hat{V}_2$ are attractive all over space, while $\phi_{1,2}$ is positive everywhere. Consequently, one finds

$$\begin{aligned}
-\Big[\langle\phi_1|\hat{V}_2|\phi_1\rangle + \langle\phi_2|\hat{V}_1|\phi_2\rangle\Big]\langle\phi_1|\phi_2\rangle &> 0 \\
\langle\phi_1|\hat{V}_2|\phi_2\rangle + \langle\phi_2|\hat{V}_1|\phi_1\rangle &< 0 \,.
\end{aligned}$$

The questions is which of the two terms dominates? For a definitive answer one has to evaluate them explicitly (at this point we finally implement $Z_1 = Z_2 = 1$). Using the form of the $1s$-orbitals,

$$\phi_i(\boldsymbol{r}) = \frac{1}{\sqrt{\pi}}\, e^{-|\boldsymbol{r}-\boldsymbol{R}_i|} \,,$$

one obtains

$$\begin{aligned}
\langle\phi_1|\hat{V}_2|\phi_1\rangle &= -\frac{1}{\pi}\int d^3r\, \frac{e^{-2|\boldsymbol{r}-\boldsymbol{R}_1|}}{|\boldsymbol{r}-\boldsymbol{R}_2|} = \langle\phi_2|\hat{V}_1|\phi_2\rangle \\
\langle\phi_1|\hat{V}_2|\phi_2\rangle &= -\frac{1}{\pi}\int d^3r\, \frac{e^{-|\boldsymbol{r}-\boldsymbol{R}_1|}\, e^{-|\boldsymbol{r}-\boldsymbol{R}_2|}}{|\boldsymbol{r}-\boldsymbol{R}_2|} = \langle\phi_2|\hat{V}_1|\phi_1\rangle \\
\langle\phi_1|\phi_2\rangle &= \frac{1}{\pi}\int d^3r\, e^{-|\boldsymbol{r}-\boldsymbol{R}_1|}\, e^{-|\boldsymbol{r}-\boldsymbol{R}_2|} \,.
\end{aligned}$$

All three integrals can be performed analytically, using prolate elliptical coordinates (see

Section 5 for details),

$$\begin{aligned}
\langle\phi_1|\hat{V}_2|\phi_1\rangle &= -\frac{1}{\pi}f^3\int_1^\infty d\xi\int_{-1}^1 d\eta\int_0^{2\pi} d\varphi\,(\xi^2-\eta^2)\,\frac{e^{-2f(\xi+\eta)}}{f(\xi-\eta)} \\
&= -2f^2\int_1^\infty d\xi\,e^{-2f\xi}\int_{-1}^1 d\eta\,(\xi+\eta)\,e^{-2f\eta} \\
&= -\frac{1}{R}\left[1-e^{-2R}(1+R)\right] \\
\langle\phi_1|\hat{V}_2|\phi_2\rangle &= -\frac{1}{\pi}f^3\int_1^\infty d\xi\int_{-1}^1 d\eta\int_0^{2\pi} d\varphi\,(\xi^2-\eta^2)\,\frac{e^{-f(\xi+\eta)}\,e^{-f(\xi-\eta)}}{f(\xi-\eta)} \\
&= -2f^2\int_1^\infty d\xi\,e^{-f2\xi}\int_{-1}^1 d\eta\,(\xi+\eta) \\
&= -e^{-R}\,[1+R] \\
\langle\phi_1|\phi_2\rangle &= \frac{1}{\pi}f^3\int_1^\infty d\xi\int_{-1}^1 d\eta\int_0^{2\pi} d\varphi\,(\xi^2-\eta^2)\,e^{-f(\xi+\eta)}\,e^{-f(\xi-\eta)} \\
&= 2f^3\int_1^\infty d\xi\,e^{-2f\xi}\int_{-1}^1 d\eta\,(\xi^2-\eta^2) \\
&= e^{-R}\left[1+R+\frac{R^2}{3}\right].
\end{aligned}$$

For the expansion in powers of $\langle\phi_1|\phi_2\rangle$ to be legitimate, R has to be sufficiently large. This condition is clearly met for $R \geq 3$ (atomic units are used here). If one analyzes

$$\begin{aligned}
\langle\phi_1|\hat{V}_2|\phi_1\rangle\,\langle\phi_1|\phi_2\rangle &= -\frac{R}{3}\,e^{-R}\left[1+\frac{3}{R}+\frac{3}{R^2}\right]+\frac{R^2}{3}\,e^{-3R}\left[1+\frac{1}{R}\right]\left[1+\frac{3}{R}+\frac{3}{R^2}\right] \\
\langle\phi_1|\hat{V}_2|\phi_2\rangle &= -R\,e^{-R}\left[1+\frac{1}{R}\right]
\end{aligned}$$

in this range, one finds the difference $E_+ - E_-$ to be negative.

A more complete picture is provided by Fig. 3. The figure shows that the symmetric combination of the atomic orbitals yields a lower energy for all R and thus represents the ground state. In fact, the energy surface of Φ_+ is attractive over a substantial range, while Φ_- produces a completely repulsive energy surface. The origin of this behavior can be traced to the individual terms in (4.5). If one inserts the explicit results into (4.5), one finds that the electrostatic repulsion between the nuclei essentially cancels with the attraction of the electron by the second nucleus, $\langle\phi_1|\hat{V}_2|\phi_1\rangle + \langle\phi_2|\hat{V}_1|\phi_2\rangle$,

$$E_\pm - \epsilon_{1s} = \frac{e^{-2R}(1+R) \pm e^{-R}(1+R+R^2/3)}{R[1\pm e^{-R}(1+R+R^2/3)]} \mp \frac{e^{-R}\,[1+R]}{[1\pm e^{-R}(1+R+R^2/3)]}\,.$$

These electrostatic energies both have the Coulombic $1/R$-dependence, but differ in sign. Consequently, the exchange term $\langle\phi_1|\hat{V}_2|\phi_2\rangle + \langle\phi_2|\hat{V}_1|\phi_1\rangle$ is decisive for bonding: it enters as an attractive term for the Φ_+ state, but in repulsive form in the case of Φ_-.

Molecular states without nodal planes perpendicular to the interatomic axis are therefore called bonding orbitals, those with such nodal planes anti-bonding. The latter states are

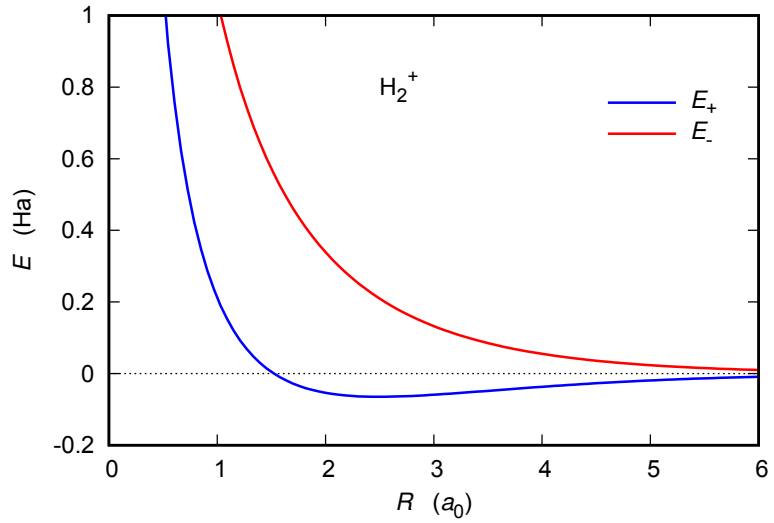

Figure 3: Energy surfaces $E_\pm - \epsilon_{1s}$, Eq.(4.5), for the H_2^+ molecule as a function of the interatomic separation R.

denoted by an additional asterisk, e.g. as π^*-orbitals. As an illustration, Fig. 4 shows the lowest bonding and anti-bonding states of the Hydrogen dimer. A second example for a bonding σ-orbital is displayed in Fig. 5. In this case, however, the molecular state is formed from two atomic p_z-orbitals. Bonding and anti-bonding variants also exist for the molecular orbitals with $m > 0$. A typical bonding π-orbital is provided by Fig. 6, together with a bonding δ-orbital.

5 Computational Details

In this Section the numerical procedures used in the program package DIAMOL are explained in some detail.

The potential (4.1) is axially symmetric with respect to the z-axis, which suggests to apply cylindrical coordinates ρ, φ, z for the solution of the KS equation (3.25). However, DIAMOL rather uses prolate spheroidal coordinates ξ, η, φ for this task, in accordance with the basis set utilized for the representation of the KS orbitals (see below). While φ is the usual azimuthal angle with respect to the z-axis ($0 \le \varphi \le 2\pi$), ξ and η are defined in terms of the distances r_1 and r_2 from the two ions to the point $\boldsymbol{r}$ (compare Fig. 2),

$$\xi = \frac{(r_1 + r_2)}{2f} \qquad 1 \le \xi < \infty \tag{5.1}$$

$$\eta = \frac{(r_1 - r_2)}{2f} \qquad -1 \le \eta \le 1\,. \tag{5.2}$$

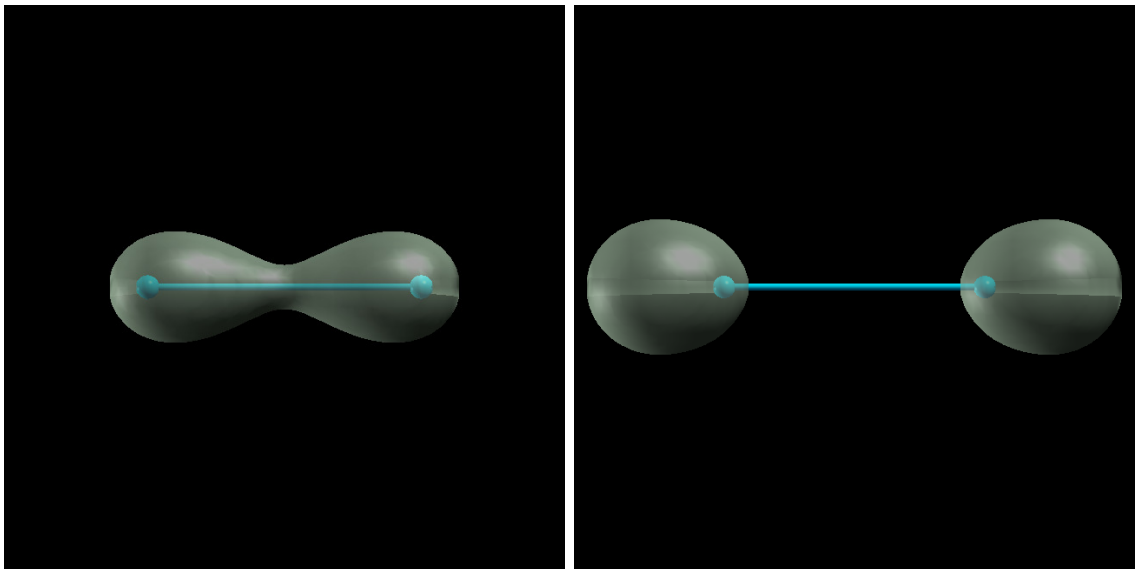

Figure 4: Bonding (left) and anti-bonding (right) σ-states of the Hydrogen dimer at $R = 1.4\,\text{Bohr}$. In the case of the bonding orbital an isosurface with density 0.9Å^{-3} is shown, for the anti-bonding orbital the density is 0.15Å^{-3}.

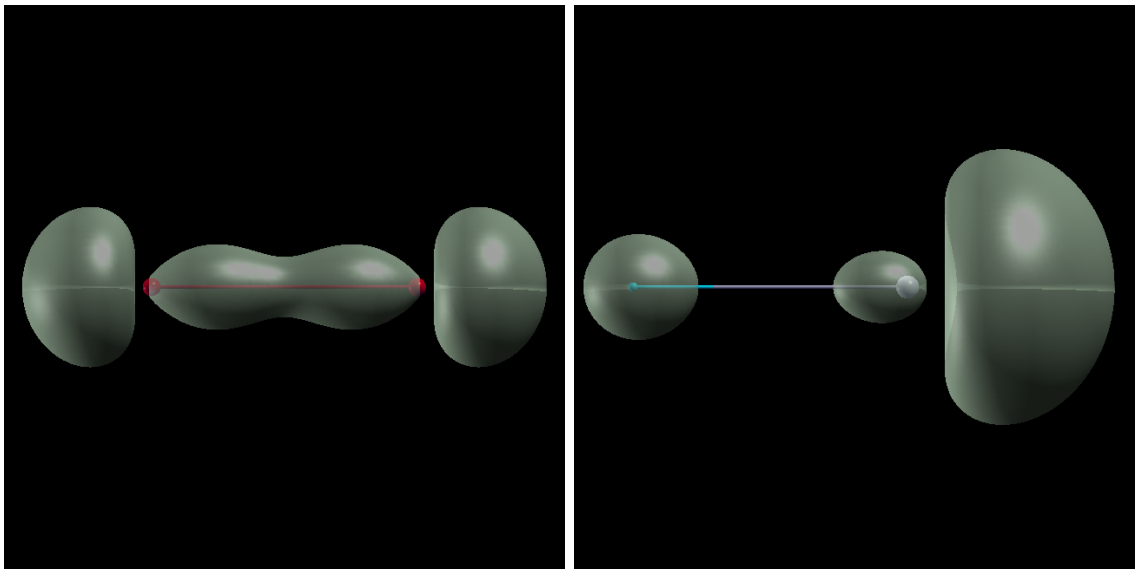

Figure 5: Left: bonding σ-state of O_2 obtained by linear combination of two p_z-orbitals ($R = 2.3\,\text{Bohr}$, density of isosurface 0.5Å^{-3}). Right: bonding σ-state of BH obtained by linear combination of the Hydrogen $1s$- with the Boron p_z-orbital ($R = 2.3\,\text{Bohr}$, density of isosurface 0.2Å^{-3}).

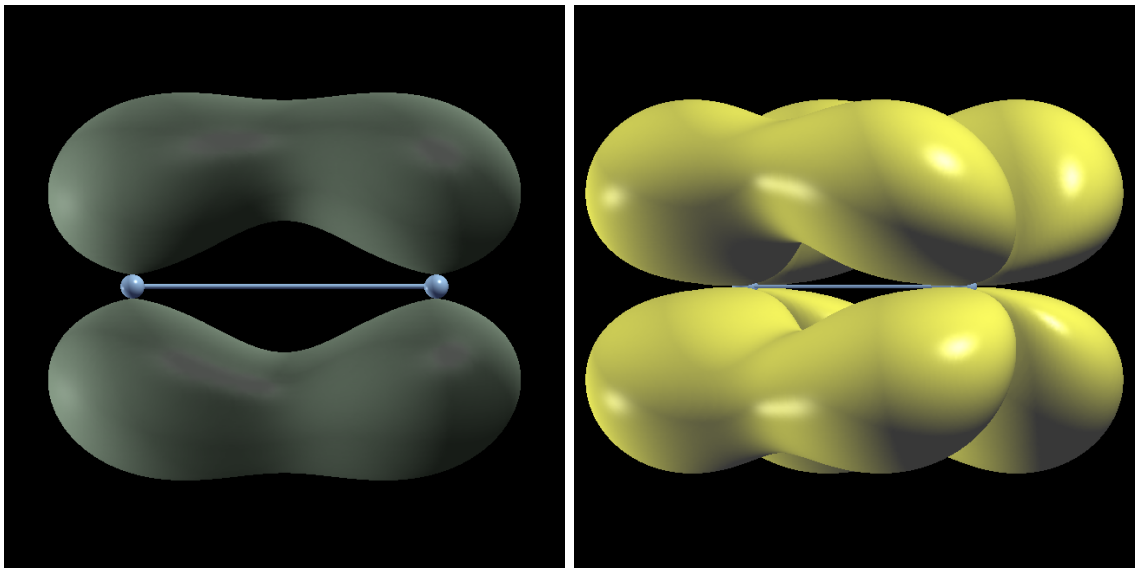

Figure 6: Left: bonding π-state of N_2 ($R = 2.0\,\text{Bohr}$, density of isosurface 0.3Å^{-3}). Right: bonding δ-state of Cr_2 obtained by linear combination of two d_{xy}-orbitals ($R = 3.2\,\text{Bohr}$, density of isosurface 0.02Å^{-3}).

The relation of ξ and η to the cylindrical coordinates ρ and z is given by

$$\begin{aligned}
\xi &= \frac{1}{2f}\left([\rho^2+(z+f)^2]^{1/2}+[\rho^2+(z-f)^2]^{1/2}\right) && (5.3)\\
\eta &= \frac{1}{2f}\left([\rho^2+(z+f)^2]^{1/2}-[\rho^2+(z-f)^2]^{1/2}\right) && (5.4)\\
\rho &= f\left[(\xi^2-1)(1-\eta^2)\right]^{1/2} && (5.5)\\
z &= f\xi\eta && (5.6)\\
d^3r &= f^3\left(\xi^2-\eta^2\right)d\xi d\eta d\varphi\,. && (5.7)
\end{aligned}$$

If one expresses the Laplacian in prolate spheroidal coordinates and uses the decomposition (4.2), with $\bar{\phi}_{jm\sigma}$ understood as a function of ξ and η, the KS equation (3.25) assumes the form

$$\left\{\hat{t}_{\xi\eta}+v_{\rm s}^{\sigma}(\xi,\eta)\right\}\bar{\phi}_{jm\sigma}(\xi,\eta) = \epsilon_{jm\sigma}\,\bar{\phi}_{jm\sigma}(\xi,\eta) \qquad (5.8)$$

with

$$\hat{t}_{\xi\eta} = \frac{-1}{2f^2(\xi^2-\eta^2)}\left[\partial_\xi(\xi^2-1)\partial_\xi+\partial_\eta(1-\eta^2)\partial_\eta-\frac{(\xi^2-\eta^2)m^2}{(\xi^2-1)(1-\eta^2)}\right]. \qquad (5.9)$$

Equation (5.8) demonstrates explicitly that the sign of m is irrelevant for the states $\bar{\phi}_{jm\sigma}$. $\phi_{j,-|m|,\sigma}$ and $\phi_{j,|m|,\sigma}$ only differ by the phase $e^{im\varphi}$ in (4.2). The subsequent discussion is therefore restricted to $m \geq 0$.

For the solution of the two-dimensional problem (5.8) the orbitals $\bar{\phi}_{jm\sigma}$ are expanded in terms of analytical basis functions ψ_{nlm},

$$\bar{\phi}_{jm\sigma}(\xi,\eta) = \sum_{n=0}^{n_{\max}} \sum_{l=m}^{m+l_{\max}} f^j_{nlm\sigma} \psi_{nlm}(\xi,\eta) \; . \tag{5.10}$$

The upper bounds $n_{\max}$ and $l_{\max}$ indicate that this expansion has to be truncated in practice. For ψ_{nlm} DIAMOL uses the non-orthogonal Hylleraas basis [8],

$$\psi_{nlm}(\xi,\eta) = (\xi^2-1)^{m/2}\, e^{-(\xi-1)/(2a)}\, L^m_n\left(\frac{\xi-1}{a}\right) P^m_l(\eta) \; , \tag{5.11}$$

where the L^m_n and P^m_l denote the generalized Laguerre polynomials and the associated Legendre functions, respectively, and a is an adjustable basis parameter (for a discussion of a see below). The Hylleraas basis is specific for two-center problems, but has the advantage that the basis functions cover the bonding region between the ions very well. With this basis the KS equation (5.8) can be recast as a generalized algebraic eigenvalue problem,

$$\sum_{n'=0}^{n_{\max}} \sum_{l'=m}^{m+l_{\max}} \left[\langle nlm|\hat{t}_{\xi\eta} + v^\sigma_{\rm s}|n'l'm\rangle - \epsilon_{jm\sigma}\langle nlm|n'l'm\rangle\right] f^j_{n'l'm\sigma} \;\; = \;\; 0 \; , \tag{5.12}$$

which has to be solved for all m which are relevant.

While the overlap and kinetic energy matrix elements $\langle nlm|n'l'm\rangle$ and $\langle nlm|\hat{t}_{\xi\eta}|n'l'm\rangle$, respectively, can be evaluated analytically [9], the potential matrix elements

$$\langle nlm|v^\sigma_{\rm s}|n'l'm\rangle \;\; = \;\; f^3 \int_1^\infty d\xi \int_{-1}^1 d\eta\, (\xi^2-\eta^2) \psi_{nlm}(\xi,\eta) v^\sigma_{\rm s}(\xi,\eta) \psi_{n'l'm}(\xi,\eta) \tag{5.13}$$

have to be calculated numerically on a suitable grid of ξ,η-points. In DIAMOL the grid is given by pairs (ξ_α,η_β), with ξ_α and η_β independently going through their respective meshes. The η-mesh could be chosen to be equidistant without much loss of accuracy. However, a minor accumulation of mesh points close to the nuclei is advantageous for larger charges Z_i and is therefore implemented in DIAMOL. The ξ-mesh has to reflect the fact that the orbitals have their maxima and nodes close to the nuclei, but fall off exponentially for large ξ. Therefore a transformation is used to concentrate more mesh points in the relevant region.

Before the integral (5.13) can be performed, the components of $v^\sigma_{\rm s}$ have to be determined. Both the Hartree and the xc-potential require knowledge of the spin-density (3.28),

$$n_\sigma(\xi,\eta) \;\; = \;\; \sum_{m=0}^{\infty} \sum_{j=1}^{\infty} \Theta(\epsilon_{N_\sigma} - \epsilon_{jm\sigma}) \left|\bar{\phi}_{jm\sigma}(\xi,\eta)\right|^2 \; , \tag{5.14}$$

where ϵ_{N_σ} is the eigenvalue of the highest occupied KS orbital for spin σ (which is determined by the number of particles N_σ with this spin). If the LDA (3.34)–(3.36) is applied — as required for the simulation — insertion of (5.14) into (3.31) directly provides $v^\sigma_{\rm xc}$ on the ξ,η-grid.

Similary, one could insert (5.14) into Eq.(3.9) to obtain $v_{\rm H}$. However, the direct integration in Eq.(3.9) is less efficient than a solution of the Poisson equation for $v_{\rm H}$,

$$\Big[\partial_\xi(\xi^2-1)\partial_\xi + \partial_\eta(\eta^2-1)\partial_\eta\Big] v_{\rm H}(\xi,\eta) \;\; = \;\; -4\pi f^2(\xi^2-\eta^2) n(\xi,\eta) \; . \tag{5.15}$$

In fact, utilizing a multipole expansion,

$$v_{\rm H}(\xi,\eta) = \frac{1}{2}\sum_{l=0}^{l_{\rm max}} (2l+1)\chi_l(\xi) P_l(\eta) \; , \tag{5.16}$$

one arrives at an ordinary differential equation for the function χ_l,

$$\Big\{\partial_\xi(\xi^2-1)\partial_\xi - l(l+1)\Big\}\chi_l(\xi) \;\; = \;\; -4\pi f^2 \int_{-1}^{1} d\eta (\xi^2-\eta^2) P_l(\eta) n(\xi,\eta) \; , \tag{5.17}$$

which is solved by a standard shooting procedure on the same ξ-grid as used for integration.

As boundary conditions for this procedure one can use

$$\left(\partial_\xi - \frac{l(l+1)}{2}\right)\chi_l(\xi)\bigg|_{\xi=1} \;\; = \;\; -2\pi f^2 \int_{-1}^{1} d\eta (1-\eta^2) P_l(\eta) n(1,\eta) \tag{5.18}$$

at the lower end of the ξ-interval. For large ξ the right-hand side of Eq.(5.17) vanishes exponentially due to the exponential decay of the density. Thus, up to exponentially decaying corrections, χ_l is asymptotically proportional to the Legendre functions of second kind, $Q_l(\xi)$ [10],

$$\chi_l(\xi) \underset{\xi\gg 1}{=} c_l \, Q_l(\xi) \; , \tag{5.19}$$

as the Q_l satisfy the asymptotic differential equation,

$$\Big\{\partial_\xi(\xi^2-1)\partial_\xi - l(l+1)\Big\} Q_l(\xi) \;\; = \;\; 0 \; ,$$

and ensure the proper boundary condition,

$$\chi_l(\xi) \underset{\xi\to\infty}{\longrightarrow} 0 \; .$$

The coefficients c_l can be evaluated by multiplying Eq.(5.17) by $P_l(\xi)$ and subsequently integrating over ξ,

$$c_l = 4\pi f^2 \int_1^\infty d\xi \int_{-1}^{1} d\eta (\xi^2-\eta^2) P_l(\xi) P_l(\eta) n(\xi,\eta) \; . \tag{5.20}$$

In this way c_0 is directly obtained as

$$c_0 = 2\frac{N}{f} \; .$$

As a result, the asymptotic boundary condition for the monopole term is

$$\chi_0(\xi_{\rm max}) = \frac{N}{f} \, \ln\left|\frac{\xi_{\rm max}+1}{\xi_{\rm max}-1}\right| \; , \tag{5.21}$$

with $\xi_{\max}$ being the maximum ξ-value of the mesh used. An explicit calculation of higher c_l can be avoided by resorting to the boundary condition

$$\left.\frac{\partial_\xi \chi_l(\xi)}{\chi_l(\xi)}\right|_{\xi=\xi_{\max}} = \left.\frac{\partial_\xi Q_l(\xi)}{Q_l(\xi)}\right|_{\xi=\xi_{\max}} . \tag{5.22}$$

Once the matrix element (5.13) is completely known, the eigenvalue problem (5.12) can be solved by use of a standard solver for matrix eigenvalue problems (DIAMOL uses a LAPACK subroutine).

It seems worthwhile to specify the numerically most stable form of the total energy (3.32),

$$\begin{aligned} E_0 \;=\; & \sum_{\sigma=\uparrow,\downarrow} \sum_{m=0}^{\infty} \sum_{j=1}^{\infty} \Theta(\epsilon_{N_\sigma} - \epsilon_{jm\sigma})\, \epsilon_{jm\sigma} + E_{\rm xc}[n_\uparrow, n_\downarrow] \\ & -\pi f^3 \int_1^\infty d\xi \int_{-1}^1 d\eta\, (\xi^2-\eta^2)\, n(\xi,\eta)\, v_{\rm H}(\xi,\eta) \\ & -2\pi f^3 \int_1^\infty d\xi \int_{-1}^1 d\eta\, (\xi^2-\eta^2)\, n_\sigma(\xi,\eta)\, v_{\rm xc}^\sigma(\xi,\eta) \;, \end{aligned} \tag{5.23}$$

where the KS equation (5.8) has been used to express the kinetic energy in terms of the KS eigenvalues. DIAMOL uses (5.23) for the calculation of E_0, rather than (3.32).

For the actual numerical integration of the matrix elements (5.13) and the total energy (5.23) DIAMOL relies on Gauss-Legendre quadrature (for both coordinates). If a suitable transformation of the ξ-grid is applied (as discussed earlier), ξ, η-grids with 64×64 grid points usually give decent results (128×128 grid points already yield very high accuracy).

Finally, some comments on the scaling parameter a of the basis (5.11) are required. a determines the location of the extrema and zeros of the L_n^m and, even more important, the asymptotic behavior of the basis functions,

$$\psi_{nlm}(\xi,\eta) \underset{\xi\gg 1}{\sim} \xi^{n+m}\, e^{-\xi/(2a)}\, P_l^m(\eta) \;.$$

This behavior has to be compared with the exact asymptotic form of the solutions of Eq.(5.8),

$$\bar{\phi}_{jm\sigma}(\xi,\eta) \underset{\xi\gg 1}{\sim} \frac{1}{\xi}\, e^{-f\sqrt{-2\epsilon_{jm\sigma}}\,\xi} \sum_{l=0}^{\infty} c_{jm\sigma}^l\, P_l^m(\eta) \;.$$

Obviously, the choice $1/a = 2f\sqrt{-2\epsilon_{jm\sigma}}$ ensures that the exponential decay of both functions is identical. One should not underestimate, however, the importance of the power of ξ in front of the exponential term: an a smaller than this choice is required in order to compensate the power law prefactors in the two functions. Moreover, the same a is applied to all molecular orbitals, so that use of an average a is necessary. The default choice for a, provided by DIAMOL, therefore aims at a balance between the various requirements on a. For the present simulations an adjustment of a is not necessary.

6 Tasks

6.1 Setup of simulation

1. Download the package DIAMOL

   `http://itp.uni-frankfurt.de/~engel/teaching/comp-simu.tar.gz`

   and extract the tar-file. A directory `comp-simu` should be created in this process. Enter into this directory.

2. Make yourself familiar with the environment: there is

   - the executable `diamol.exe`,
   - an input file called `modein.diamol`, which provides all technical parameters for `diamol.exe` which do not depend on the molecule to be calculated,
   - a directory `in`, in which you find specific input files for several molecules,
   - a shell script `run.diamol`, which can be used for a single calculation with `diamol.exe` (it sets all relevant shell variables for IO and runs the program),
   - a shell script `run.diamol.list`, which can be used for series of calculations with `diamol.exe` (it starts `run.diamol` for all molecules listed in the file given as an argument — an example is the file `list` — and, for given molecule, all interatomic separations provided in the file `run/list.molecule_name`),
   - a directory `run` with the example `run/list.h_2` for the file of interatomic separations required by `run.diamol.list`,
   - an empty directory `out` to which `run.diamol.list` writes out results,
   - a shell script `morsefit` and the accompanying executable `morsefit.exe`, which allow you to fit some data set to the Morse potential (the most simple representation of the energy surface resulting from covalent bonds), assuming the data to be in two-column format with each line containing one pair $(R, E(R))$,
   - a directory `reference_data`, in which you find reference results for the energy surface of the Hydrogen dimer.

3. Make yourself familiar with `modein.diamol`: this file contains a number of parameters for which the default values in the file should be left untouched, i.e. `NITMAX`, `LINMIX`, `MODESA`, `RBOUND`, `MODENX`, `DENASY`, `HYBMIX`, `NSTART`, `MBAMP2`, `NX`, `EIGCUT`, `TOLDEG`. The parameters relevant for the simulation are:

   - `TOLPOT` controls the accuracy of the self-consistent KS iteration. The value of `1.E-5` should be fine for your simulation.
   - `NU` and `NV` define the number of grid points of the ξ- and η-grids, respectively. The choice 64×64 should be fine.

- MODEX and MODEXO determine which exchange functional is applied in (i) the self-consistent KS iteration (MODEX) and (ii) an *a posteriori* evaluation with the states obtained in step (i) (MODEXO). Such an *a posteriori* evaluation is only performed, if MODEXO differs from MODEX. MODEC and MODECO are analogous parameters for the correlation functional. You should use the LDA for both components, MODEX=MODEXO=MODEC=MODECO=11. MODEC=11 corresponds to the parameterization of the LDA correlation functional of Ref. [4].
- MODEST determines in which way the program sets up the starting potential. For MODEST=0 an internal guess is used, for MODEST=1 the program uses the output of a previous run (when applied properly). For the first run for any interatomic separation you have to use MODEST=0. When repeating calculations (e.g. for plotting), you may want to use MODEST=1.
- MODEPR controls the amount of output generated. In particular, MODEPR=1 provides additional diagnostic printout (e.g. for tracking some failure) and MODEPR=8 lets the program print out the density of state number NPLOT of spin SPLOT (UP or DN) in a cubic box with corners (±XPLOT,±XPLOT,±XPLOT), using a format suitable for plotting with the program Xcrysden. Plotting of densities with Xcrysden is explained at http://www.xcrysden.org/doc/density.html.

4. Make yourself familiar with the specific input files for molecules such as in/h_2: they contain
   - a free comment on the molecule in the first line;
   - all crucial parameters on the molecule in the second line, i.e.
     - a string % which allows to set the interatomic separation R from outside of the file via the stream editor sed,
     - the nuclear charges ZNUC1 and ZNUC2 and the number of states NORBIT to be calculated,
     - the parameters MODEMU and MODEMD, which are not required for your simulation and should be left untouched;
   - NORBIT lines providing the m quantum numbers and the occupations (1.0 or 0.0 for the present purpose) of all states to be calculated, spin-up on the left-hand side and spin-dn on the right — for any particular m the program associates the first line with the energetically lowest molecular orbital with this m, the second line with the energetically next state and so on, for both spins independently;
   - the mixing ratio WEIGHT, which you should leave at the default value of 0.35;
   - finally a line which determines the basis set, i.e.
     - the basis parameter A (setting this input to 0.0 lets the program choose a default value, which is fine for the present purpose),
     - the highest index NBAMAX= $n_{\max}$ of the Laguerre polynomials in the basis (5.10),
     - the highest index LBAMAX= $l_{\max}$ of the associated Legendre functions in the basis (5.10),

- the highest m quantum number `MBAMAX` for which (5.8) is solved,
- the highest multipole `LHMAX` included in the multipole expansion (5.16),
- the parameters `NNODE` and `MNODE`, which allow a fine-tuning of `A` on the basis of the default value (which is irrelevant for your simulations) as well as the parameter `LHSTEP`, which can be used to manipulate the multipole expansion (5.16) (which is also irrelevant for your simulations).

5. Make yourself familiar with the shell scripts `run.diamol`, `run.diamol.list` and `morsefit`

   - The handling of these shell scripts is explained in the scripts themselves.

6.2 Work plan

1. As a warmup and to ensure that you can correctly handle the program, calculate the energy surface of H_2. Suitable input files are found in the directory `in` (called `h_2` for the hydrogen dimer and `h` for the hydrogen atom), reference results obtained with this input are provided in the directory `reference_data`. From the content of this directory make yourself clear which steps are required for generating an energy surface.

2. Calculate the ground and lowest excited state energy surface of CO (according to experiment). An input file for the ground state can be found in the directory `in` (called `co`). Check the literature which many-electron state is the first excited state of CO, in order to set up the input file. To understand the structure of this input file first think about a corresponding file for an excited hydrogen atom.

3. In order to calculate the energy surfaces of both CO states set up input files for the isolated carbon and oxygen atoms and calculate their ground states, placing the atoms at the same positions in space as in the molecule.

4. Generate data files with the energy surfaces of these states (in the two-column format $(R, E(R))$) by using `grep` to collect the ground state energies of the output files obtained for the various internuclear separations. Evaluate the spectroscopic constants for both energy surfaces with `morsefit`.

5. Determine the nature of the bonding molecular orbitals for both surfaces by plotting them with `Xcrysden` (consult the tutor for the details of handling `Xcrysden`, see also `http://www.xcrysden.org/doc/density.html`).

6.3 Report

In your report on the simulation you should in particular cover the following aspects:

1. Explain the physics behind the Born-Oppenheimer approximation. When does it break down and why?

2. What are the spectroscopic constants of a diatomic molecule and how are they related to the energy surface?

3. Which non-electronic excitations are possible in a diatomic molecule and how are they related to the spectroscopic constants?

4. Which bond types exist for diatomic molecules?

5. Discuss all your results, such as the energy surfaces and the character of the bonding orbitals for both states. Which error estimates for your results can you give?

There is no need to give an introduction to DFT in your report. The same applies to the technical details of DIAMOL.

References

[1] E. Engel. Quantum molecular dynamics. `https://itp.uni-frankfurt.de/~engel/teaching/qmd.pdf`, 2015.

[2] A. S. Dawydow. *Quantenmechanik*. VEB Deutscher Verlag der Wissenschaften, Berlin, 1978.

[3] E. Engel and R. M. Dreizler. *Density Functional Theory: An Advanced Course*. Springer, Berlin, 2011.

[4] S. H. Vosko, L. Wilk, and M. Nusair. *Can. J. Phys.*, 58:1200, 1980.

[5] J. P. Perdew and A. Zunger. *Phys. Rev. B*, 23:5048, 1981.

[6] G. Ortiz and P. Ballone. *Phys. Rev. B*, 50:1391, 1994.

[7] H. Haken and H. Ch. Wolf. *Molekülphysik und Quantenchemie*. Springer, Berlin, 1998.

[8] E. A. Hylleraas. *Z. Phys.*, 71:739, 1931.

[9] J. Eichler and U. Wille. *Phys. Rev. A*, 11:1973, 1975.

[10] M. Abramowitz and I. A. Stegun, editors. *Handbook of Mathematical Functions*. Dover, New York, NY, 1965.